Hindawi Publishing Corporation
International Journal of Polymer Science
Volume 2016, Article ID 5368602, 10 pages
http://dx.doi.org/10.1155/2016/5368602

Research Article

Photoinduced Copolymerization of APMP-MMA: The Role of Reactive Hindered Amine APMP

Ting Zhang,[1,2] Liuwa Fu,[1] Zhikang Chen,[1] Yanyan Cui,[1] and Xiaoxuan Liu[1]

[1]*Guangdong Provincial Key Laboratory of Functional Soft Condensed Matter, Department of Polymeric Materials and Engineering, School of Materials and Energy, Guangdong University of Technology, Guangzhou 510006, China*
[2]*College of Chemistry and Environment, Minnan Normal University, Zhangzhou, Fujian 363000, China*

Correspondence should be addressed to Xiaoxuan Liu; p-xxliu@gdut.edu.cn

Received 8 February 2016; Accepted 30 May 2016

Academic Editor: Atsushi Sudo

4-Acryloyl-1,2,2,6,6-pentamethyl-piperidinol (APMP) is a reactive hindered amine that prolongs the service life of the polymeric materials and exhibits high stability, good resistance to extraction, and low toxicity. In this paper, a photoinduced free radical copolymerization of APMP and methyl methacrylate (MMA) is accomplished at ambient temperature in solution. APMP plays a key role in the copolymerization, owing to the nitroxides generated in situ from the moiety of 1,2,2,6,6-pentamethyl-piperidine under UV irradiation, and mediates the copolymerization, which is confirmed by the linear kinetics. With the increment of initial monomer feed ratios of APMP/MMA, both the copolymerization rate and the average molecular weight increase. According to the reactivity ratios from the extended Kelen-Tüdos (KT) method at high conversion by ^{1}H NMR spectroscopy, a nonlinear model is established and the sequential distribution in the copolymers is also investigated. The dispersion of APMP units is regulated by the feed ratios and reactivity ratios.

1. Introduction

Comparing with thermal process, the photoinduced polymerization is a generally economical and convenient technology that offers a number of advantages, including ambient temperature processing, fast curing, and spatial and temporal control over the polymerization [1]. It has been used in extensive application, such as coating industry, paints or printing inks, adhesives, composite materials, and dental restorative formulations [2]. In a photoinduced polymerization, the monomers determine the polymers with the desired physical and chemical properties, which will be in evaluation of the specific final applications.

Acrylates are often used as monomers in photoinduced polymerization for their high activity. The acrylate monomer with functional groups can provide plenty of excellent characteristics. For example, the acrylates containing fluorine provide the polymers with unique surface properties in high thermal stability, good chemical inertness and oxidative stability, superior weatherability, oil and water repellency, low flammability, and good biocompatibility as well as low refractive index [3, 4]. The acrylates containing silicon enhanced the adhesion to the surface and extraction resistance in coating [5]. The acrylates containing azobenzene group exhibit excellent photoelectric property, which is considered as a light-responsible smart monomer [6]. Acrylates are versatile when modified by the functional groups. Herein, an acrylate monomer containing a hindered amine group 1,2,2,6,6-pentamethyl-piperidine, called 4-acryloyl-1,2,2,6,6-pentamethyl-piperidinol (APMP), is introduced.

The oxidation of APMP in a photoinduced polymerization has been shown in Scheme 1, where the product is 4-acryloyl-2,2,6,6-tetramethyl-piperidinyl-1-oxyl (A-TEMPO). Since 2,2,6,6-tetramethyl-piperidinyl-1-oxyl (TEMPO) is well known for the hindered stable radical, excellent capacity in trapping active radicals [7], and fast electron transfer, the molecule structures with TEMPO moiety are used as antioxidants [8, 9], hindered amine light stabilizers (HALS) [10], molecular probes [11], spin labels [12], mediators for the controlled/living polymerization [13], and reactive redox mediators in organic radical battery [14, 15].

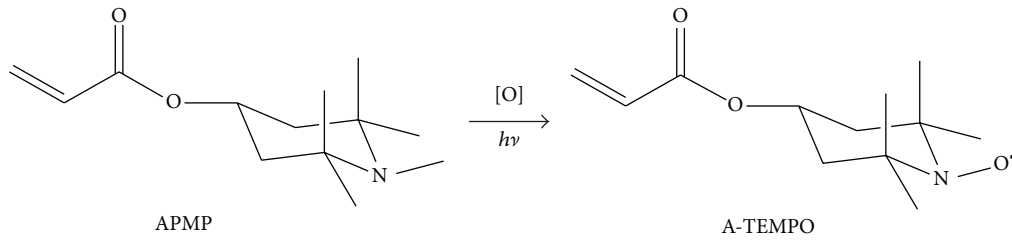

APMP A-TEMPO

Scheme 1: Structure of APMP and A-TEMPO.

As a reactive hindered amine, APMP can incorporate into the polymer by photoinduced radical polymerization to show higher stability, more resistance to extraction, and lower toxicity [16–20]. It has been proved that the UV-curing coating which copolymerized APMP exhibits higher photostability than those with the commercial light stabilizer Tinuvin292 [21]. When APMP is copolymerized with other monomers, the reactivity ratios of the system become important for that they are the quantitative values to predict the copolymer composition for any starting feed to understand the kinetic and mechanistic aspects of copolymerization [22]. It has attracted certain interest in the living radical copolymerization [23]. The determination of monomer reactivity ratio is carried out by the methods of Mayo-Lewis [24], Fineman-Ross [25], Kelen-Tüdos, and extended Kelen-Tüdos [26–28].

In this paper, the reaction kinetics in the photoinduced copolymerization of APMP with methyl methacrylate (MMA) have been investigated. By the analysis of ^{1}H NMR spectra, the reactivity ratios of the two monomers at high monomer conversions and the sequential distribution of poly(APMP-*co*-MMA) have been obtained [29]. The study of this photoinduced copolymerization could be the guidance for the application of APMP derivatives as the reactive light stabilizers.

2. Experimental Section

2.1. Materials. 4-Acryloyl-1,2,2,6,6-pentamethyl-piperidinol (APMP) was prepared according to the literature [30, 31]. Darocur1173 (2,2-dimethyl-2-hydroxy-acetophenone, BASF) was used as a photoinitiator without further purification. Methyl methacrylate (MMA) and benzene were distilled before application.

2.2. APMP-MMA Copolymerization. APMP and Darocur1173 (2.5 wt.% of the total monomer dosage) were accurately weighed and dissolved in benzene. The feeding molar ratios of APMP/MMA (M_1/M_2) for the copolymerization system were as follows: 10/90, 30/70, 50/50, 70/30, and 90/10. The solution (3 mL) with 50 wt.% monomers was charged through a syringe into a polyethylene bag, which was quickly sealed up with a plastic sealer after the air inside had been driven out by lightly pressing.

The sample bag was irradiated at ambient temperature under the light intensity of 2.1 mW·cm^{-2} measured by a UV radiometer (Photoelectric Instrument Factory of Beijing Normal University, China), which was at a distance of 20 cm from the UV radiation photoreactor (Mejiro Genossen CHG-200). After irradiation, the polymer was purified from the mixture using two or three times the reprecipitation with water/acetone and dried for 12 hrs in vacuum at 50°C subsequently. Percentage of monomer conversions was obtained gravimetrically.

2.3. Characterization of Poly(APMP-co-MMA) Copolymers. The structures and compositions of poly(APMP-*co*-MMA) had been characterized using ^{1}H NMR spectroscopy, recorded at 400 MHz on a Varian Unity 400 NMR from acetone-d_6 or chloroform-d_6 solution at ambient temperature. Gel permeation chromatography (GPC) was performed using a Waters 515 instrument equipped with a 510 Waters pump and a RI-410 refractometer. A polystyrene gel column was used with THF as the eluent at 40°C.

APMP monomer: ^{1}H NMR (400 MHz, acetone-d_6, δ, ppm): 1.15–0.89 (*m*, 12H, 4 -CH_3), 1.56–1.37 (*m*, 2H, -CH_2-), 1.95–1.66 (*m*, 2H, -CH_2-), 2.18 (*d*, J = 4.65 Hz, 3H, >N-CH_3), 5.20–4.90 (*m*, 1H, >CH-), 5.73 (*d*, J = 10.43 Hz, 1H, =CH-), 6.03 (*dd*, J = 17.34, 10.40 Hz, 1H, =CH-), 6.31 (*d*, J = 17.29 Hz, 1H, =CH-).

3. Results and Discussion

3.1. APMP-MMA Copolymerization. The APMP-MMA copolymerization was performed under the light irradiation at ambient temperature. The total monomer conversion changed with irradiation time and the kinetics was shown in Figure 1. From Figure 1(a), it revealed that the total monomer conversion was 0.605 in 60 min, where the feed ratio was 10/90 of APMP/MMA. When the feed ratio was 90/10, the conversion reached 0.609 only in 8 min. It demonstrated that, with the higher feed ratio of APMP, the conversion increased in a shorter time. Figure 1(b) exhibited that the reaction kinetics of the APMP-MMA copolymerization were linear, owing to the nitroxides that oxidized by the dissolved oxygen in solution under irradiation from APMP monomers and APMP units in the copolymers. The nitroxides exhibited a good performance to trap the radicals and mediated the polymerization [32].

However, the molecular weight distribution (MWD) of the copolymers was not the same as those in other nitroxides mediated polymerization [13]. The MWD of the copolymers from the GPC had a wide distribution that was shown in Table 1. With the increment of the feed ratios of APMP/MMA, the average molecular weight increased

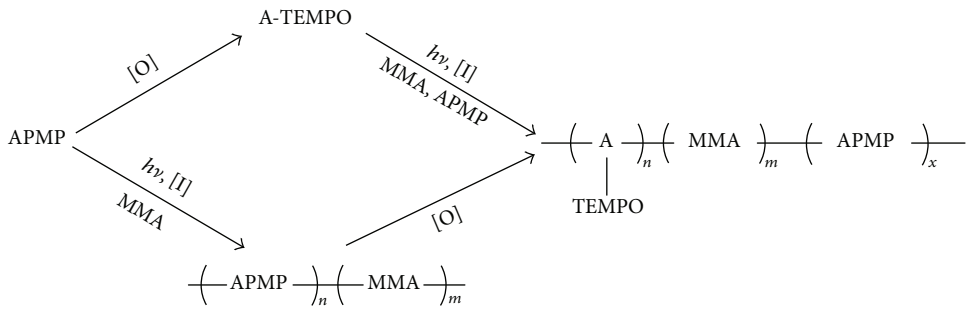

Scheme 2: The assumption of the role of APMP in the photoinduced copolymerization.

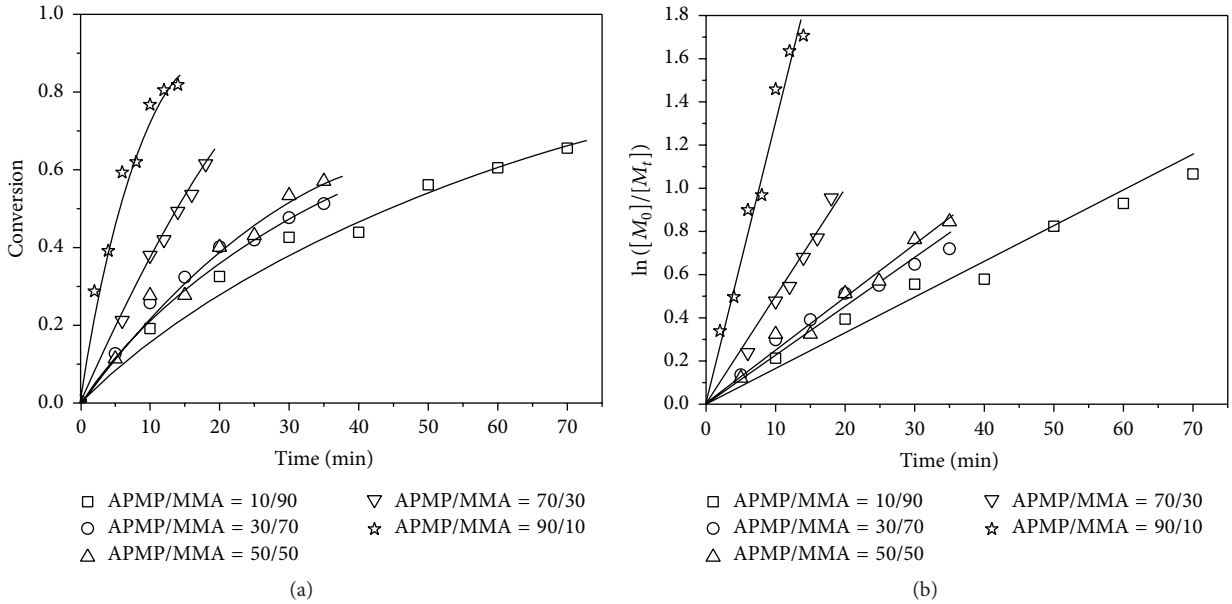

Figure 1: The relationships of (a) total monomer conversion with irradiation time and (b) the reaction kinetics in the photoinduced APMP-MMA copolymerization.

Table 1: The GPC data for poly(APMP-co-MMA).

APMP/MMA	$\overline{M_n}$ ($\times 10^4$)	$\overline{M_w}$ ($\times 10^4$)	MWD
10/90	2.37	8.03	3.40
30/70	6.61	29.21	4.42
50/50	6.32	11.13	1.76
70/30	12.53	35.61	2.84
90/10	31.88	44.38	1.39

dramatically but with different MWD. It was inferred that the nitroxides were generated from both the APMP monomer and APMP units in the copolymers. When the APMP units in the copolymer were generated into nitroxides, they could trap the propagating radicals to form branched dormant chains. The concentration of branched dormant chains increased with the concentration of AMPM in the copolymerization. Therefore, the copolymer had a high average molecular weight when the feed ratios of APMP/MMA increased. The assumption was shown in Scheme 2.

3.2. ^{1}H NMR Spectra of Poly(APMP-co-MMA). The ^{1}H NMR spectra of the poly(APMP-co-MMA) where total monomer conversion was about 0.4 were shown in Figure 2. It was shown that, with the decrement of APMP feed ratio, the peaks at 0.85 ppm which indicated the *rr* trials of MMA units [29] increased dramatically. When the feed ratio of APMP/MMA was no more than 50/50, MMA tended to form syndiotactic units. Meanwhile, the minor peaks at 0.9~1.0 ppm suggested that some MMA formed random *mr* trials. The implication for isotatic *mm* trials of MMA units at 1.2~1.3 ppm was little [33, 34].

In Figure 3, the ^{1}H NMR spectra in the range of 0.8~1.2 ppm at different total monomer conversion for each APMP-MMA copolymerization system were shown. The peaks at 0.85 ppm enlarged evidently with the increment of total monomer conversion from Figures 3(a) and 3(b) and kept nearly constant in Figure 3(c); no peaks were found at 0.85 ppm in Figures 3(d) and 3(e). It could be deduced that when the feed ratio of APMP/MMA was less than 50/50, most of the APMP monomer is exhausted at relatively lower total monomer conversion and the rest of the MMA

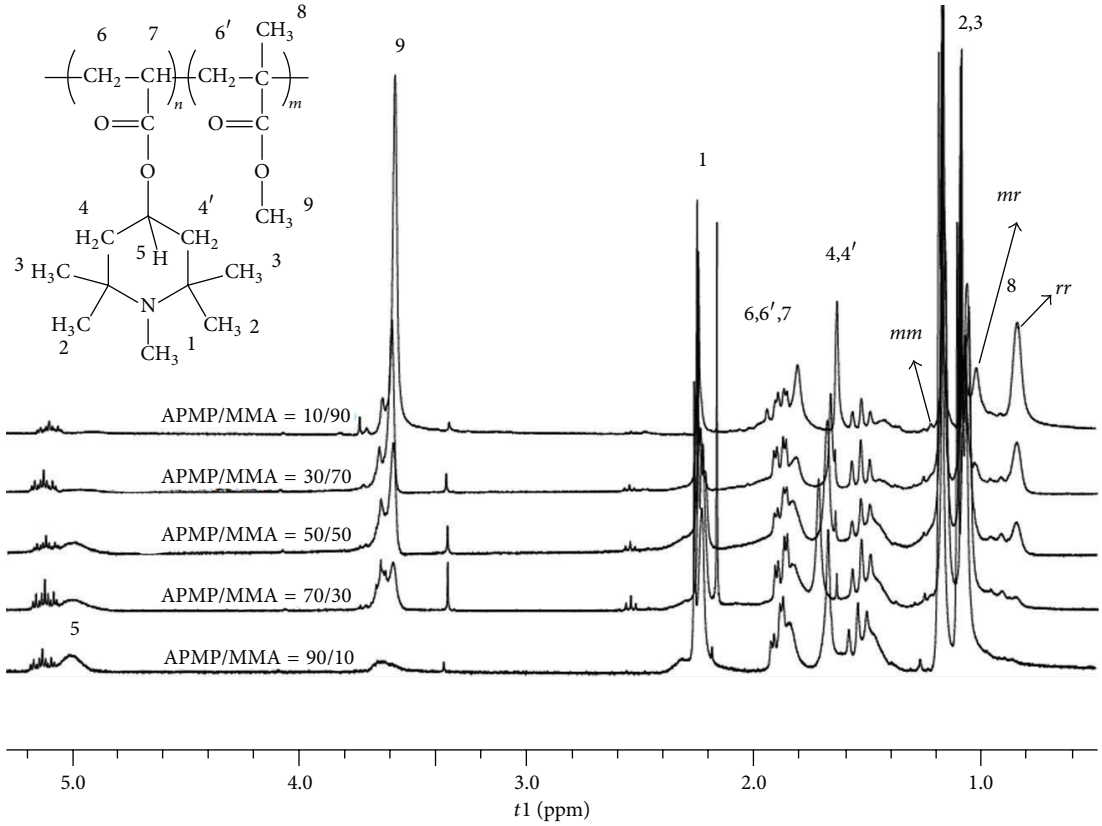

Figure 2: ^{1}H NMR spectra of poly(APMP-*co*-MMA)s with different molar ratios.

monomer had to form homopolymerized segments in the chain propagation. When the feed ratio of APMP/MMA equaled 50/50, the feed ratio approached the azeotropic copolymerization. While the feed ratios were larger than 50/50, the MMA monomer copolymerized with APMP, with single MMA unit dispersing in the copolymer backbone.

3.3. Determination of Reactivity Ratios. The absorbing band of -OCH_3 (δ = 3.6 ppm) was selected as a quantitative standard of methacrylate component due to the fact that there were no interfere bands in the nearby region, while the absorbing bands of all protons (δ < 5.2 ppm) except for -OCH_3 were as a standard of APMP component. Assuming the peak area of each proton was a and each -OCH_3 in MMA was A in the copolymer, it could be concluded that A equaled $3a$ for there were 3 -H atoms in -OCH_3 moiety. In other words, the amount of MMA units that were in the copolymer was $A/3$. When the other peak area of the absorbing bands of all protons except for -OCH_3 was R, it could be inferred that the APMP units in the copolymer were $[R - (8 - 3)a]/23$ for there were 23 -H atoms in a APMP unit and 8 -H atoms in a MMA unit. Therefore, the molar ratio of APMP units and MMA units in the copolymers was shown as

$$\frac{d[M_1]}{d[M_2]} = \frac{(R - 5A/3)/23}{A/3} = \frac{3R/A - 5}{23}. \quad (1)$$

From the results of (1), the composition of F_1 (APMP units) and F_2 (MMA units) in the copolymers was obtained by (2). The composition data of poly(APMP-co-MMA) estimated from ^{1}H NMR were listed in Table 2:

$$F_1 = \frac{d[M_1]}{d[M_1] + d[M_2]} = \frac{1}{1 - (d[M_1]/d[M_2])^{-1}} = 1 - F_2. \quad (2)$$

In Table 2, it was shown that F_1 (APMP units) decreased with the increment of total monomer conversion when the initial feed ratios of APMP/MMA were 10/90 and 30/70. Meanwhile, the trends of F_2 (MMA units) versus conversion were opposite to F_1 versus conversion. However, F_1 and F_2 changed a little while the conversion increased when the initial feed ratios were no less than 50/50.

The composition F_1 of APMP in the copolymers could be obtained according to the initial feed ratio of APMP ($f_{1,0}$), which was shown in Figure 4. When the initial feed ratio of APMP was 0.57, it would be an azeotropic copolymerization of APMP with MMA.

The extended Kelen-Tüdos (K-T) methods (see (3)) are applicable for the manipulation of high conversion. In (3), $X = [M_1]/[M_2]$ is the feed ratio and $Y = d[M_1]/d[M_2]$ is the molar ratio of monomers M_1 and M_2 contained in the copolymers; W is the conversion of the copolymerization, which is estimated by gravimetric measurement; $\mu = \mu_2/\mu_1$

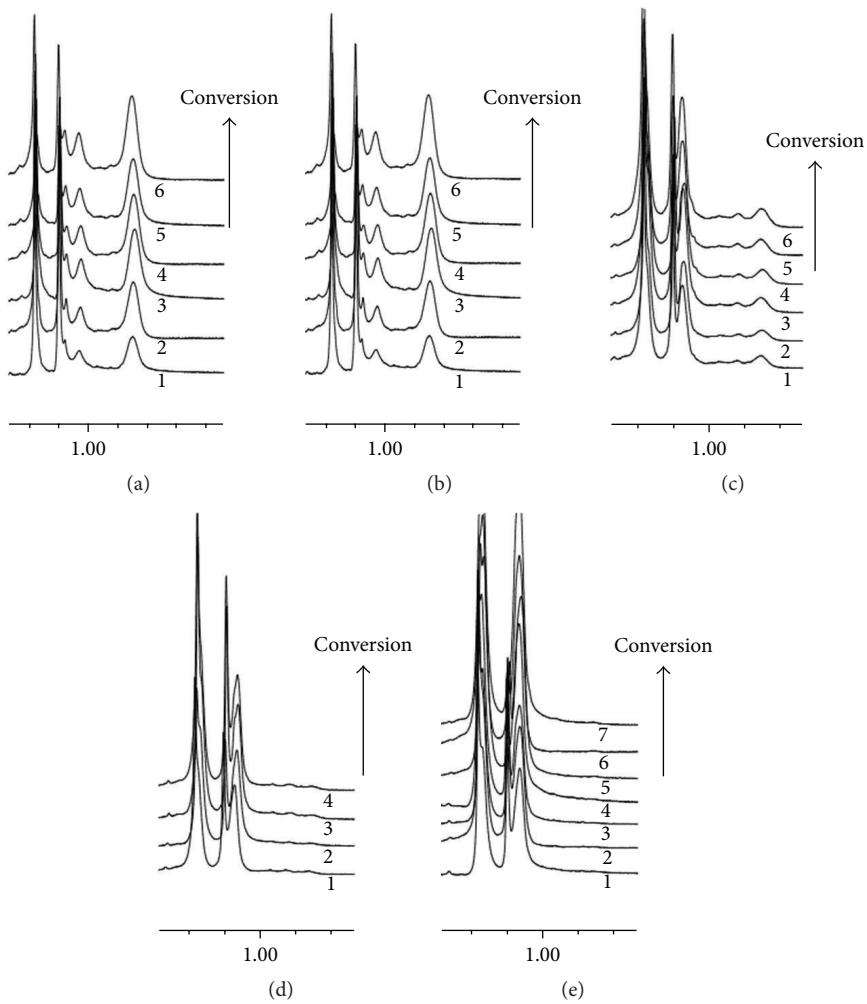

Figure 3: The ^{1}H NMR spectra of the copolymers with different total monomer conversion in each initial feed ratio of APMP/MMA system: (a), (b), (c), (d), and (e) for 10/90, 30/70, 50/50, 70/30, and 90/10, respectively.

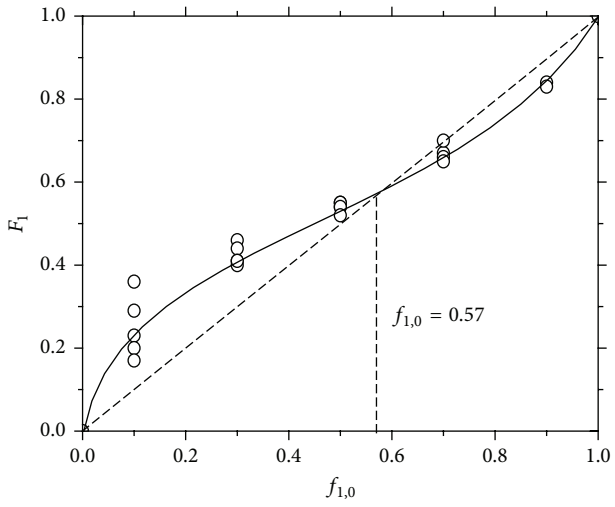

Figure 4: F_1 as a function of $f_{1,0}$ plots for photoinduced APMP-MMA copolymerization.

stand for the molecular weight ratio of monomers, in which μ_1 and μ_2 are the molecular weights of monomers M_1 and M_2, respectively. $F_{\max}$ and $F_{\min}$ are the highest and lowest values calculated from the experimental data:

$$\eta = \left(r_1 + \frac{r_2}{\alpha}\right)\xi - \frac{r_2}{\alpha},$$

$$\eta = \frac{G}{\alpha + F},$$

$$\xi = \frac{F}{\alpha + F},$$

$$\alpha = \left(F_{\max} \times F_{\min}\right)^{1/2}$$

$$F = \frac{Y}{Z^2},$$

$$G = \frac{Y - 1}{Z},$$

Table 2: Composition data of poly(APMP-co-MMA) estimated from ^{1}H NMR spectra.

Number	Feed ratio (APMP/MMA)	$f_{1,0}$	Conv.	R/A	$d[M_1]/d[M_2]$	F_1 (APMP)	F_2 (MMA)
AM19-1	10/90	0.1	0.192	4.63	0.55	0.36	0.64
AM19-2		0.1	0.325	3.80	0.42	0.29	0.71
AM19-3		0.1	0.462	3.68	0.30	0.23	0.77
AM19-4		0.1	0.439	3.34	0.25	0.20	0.80
AM19-5		0.1	0.561	3.41	0.26	0.20	0.80
AM19-6		0.1	0.605	3.47	0.25	0.20	0.80
AM19-7		0.1	0.656	3.21	0.20	0.17	0.83
AM37-1	30/70	0.3	0.127	8.25	0.86	0.46	0.54
AM37-2		0.3	0.258	7.68	0.78	0.44	0.56
AM37-3		0.3	0.324	7.60	0.77	0.44	0.56
AM37-4		0.3	0.402	6.95	0.69	0.41	0.59
AM37-5		0.3	0.420	6.88	0.68	0.40	0.60
AM37-6		0.3	0.477	6.91	0.68	0.41	0.59
AM37-7		0.3	0.513	7.01	0.70	0.41	0.59
AM55-1	50/50	0.5	0.277	11.09	1.23	0.55	0.45
AM55-2		0.5	0.277	10.82	1.19	0.54	0.46
AM55-3		0.5	0.401	10.89	1.20	0.55	0.45
AM55-4		0.5	0.431	10.62	1.17	0.54	0.46
AM55-5		0.5	0.534	9.94	1.08	0.52	0.48
AM55-6		0.5	0.571	9.94	1.08	0.52	0.48
AM73-1	70/30	0.7	0.420	17.14	2.02	0.67	0.33
AM73-2		0.7	0.493	19.69	2.35	0.70	0.30
AM73-3		0.7	0.537	16.53	1.94	0.66	0.34
AM73-4		0.7	0.615	16.09	1.88	0.65	0.35
AM91-1	90/10	0.9	0.287	40.78	5.10	0.84	0.16
AM91-2		0.9	0.394	38.20	4.77	0.83	0.17
AM91-3		0.9	0.569	39.23	4.9	0.83	0.17
AM91-4		0.9	0.608	38.51	4.81	0.83	0.17

$$
\begin{aligned}
Z &= \frac{\lg(1-\zeta_1)}{\lg(1-\zeta_2)},\\
\zeta_2 &= \frac{W(\mu+X)}{\mu+Y},\\
\zeta_1 &= \frac{\zeta_2 Y}{X},\\
X &= \frac{[M_1]_0}{[M_2]_0},\\
Y &= \frac{d[M_1]}{d[M_2]}.
\end{aligned}
\tag{3}
$$

The corresponding η versus ξ plots were shown in Figure 5. From the values of the slope and intercept of the fitting line in Figure 5, it was obtained that $r_1 = 0.353$ and $r_2 = 0.168$. The results showed that both APMP and MMA had a tendency toward alternating copolymerization in the copolymerization system.

3.4. A Nonlinear Model for APMP-MMA Copolymerization. Skeist [35] developed a relation to describe the drift in monomer feed ratio in respect of the course of a copolymerization, which Meyer and Lowry [36] later derived to [37]

$$
\begin{aligned}
1-\frac{M}{M_0} = X &= 1-\left(\frac{f_1}{f_{1,0}}\right)^{\alpha}\left(\frac{1-f_1}{1-f_{1,0}}\right)^{\beta}\left(\frac{f_{1,0}-\delta}{f_1-\delta}\right)^{\gamma}\\
\alpha &= \frac{r_2}{1-r_2},\\
\beta &= \frac{r_1}{1-r_1},\\
\gamma &= \frac{1-r_1 r_2}{(1-r_1)(1-r_2)},\\
\delta &= \frac{1-r_2}{2-r_1-r_2},
\end{aligned}
\tag{4}
$$

where $f_{1,0}$ and f_1 represented the initial monomer feed composition and the feed composition of M_1 at overall monomer conversion X, respectively. The equation described the drift of monomer feed composition as each monomer was

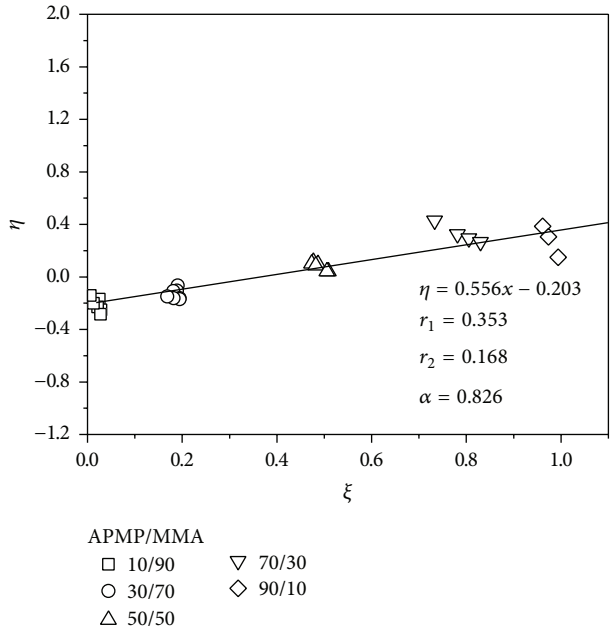

Figure 5: Relationship of η-ξ in the extended KT method for photoinduced APMP-MMA copolymerization.

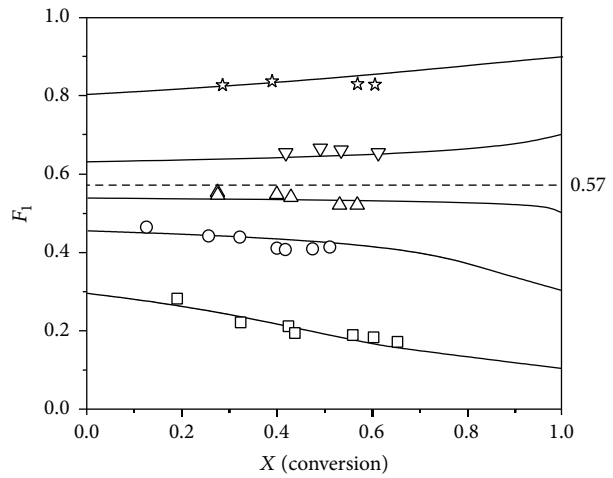

Figure 6: Cumulative copolymer composition of M_1 (APMP) versus total monomer conversion for the photoinduced copolymerization of APMP-MMA with feed ratios $f_{1,0}$ of (□) 0.1, (○) 0.3, (△) 0.5, (▽) 0.7, and (☆) 0.9.

consumed at different rates during the copolymerization. The cumulative copolymer composition of APMP (F_1) depended on the overall conversation X, which was shown in

$$F_1 = \frac{[M_1]_0 - [M_1]}{[M]_0 - [M]} = \frac{f_{1,0} - (1 - X) f_1}{X}. \quad (5)$$

The cumulative copolymer composition versus total monomer conversion for the photoinduced APMP-MMA copolymerization was shown in Figure 6, where the plots were obtained from the experimental results of the copolymerization and the lines obtained from the reactivity ratios ($r_1 = 0.353$, $r_2 = 0.168$) by (4) and (5). The constant composition of the APMP in the copolymers would be 0.57 when the azeotropic copolymerization would occur with the initial feed ratio of APMP of 0.57. In Figure 6, it was illustrated that the plots of F_1 versus X were dispersed on the lines, which indicated that the nonlinear model from (4) and (5) was fit for the photoinduced copolymerization of APMP-MMA. In other words, the reactivity ratios that were from the extended KT method were confirmed in the copolymerization.

3.5. Sequential Distribution of Poly(APMP-co-MMA). When x was the sequential number of M_1 and M_2, the probabilities to have the xM_1 and xM_2 in the copolymer were presented by the molar ratios $(N_1)_x$ and $(N_2)_x$, which were obtained by

$$(N_1)_x = (P_{11})^{x-1} P_{12},$$
$$(N_2)_x = (P_{22})^{x-1} P_{21}, \quad (6)$$

where $P_{11} = r_1[M_1]/(r_1[M_1] + [M_2])$, $P_{12} = [M_2]/(r_1[M_1] + [M_2])$, $P_{21} = [M_1]/(r_2[M_2] + [M_1])$, and $P_{22} = r_2[M_2]/(r_2[M_2] + [M_1])$. $P_{11}(P_{22})$ and $P_{12}(P_{21})$ denoted the probabilities of M_1 and M_2 unit in the copolymers, respectively. The sequential distribution of APMP units was greatly affected by the feed ratios and the reactivity ratios. When $r_1 = 0.353$ and $r_2 = 0.168$, the number of the sequence lengths xM_1 (APMP units) and xM_2 (MMA units) was illustrated in Figure 7. For $f_{1,0} = 0.1$, it was about 98.8% of unitary APMP contained in the backbone of poly(APMP-*co*-MMA). The results showed that unitary APMP units were dispersed in the MMA chains. For $f_{1,0} = 0.3$, the chance to have unitary APMP was 88.6% and unitary MMA was 62.7% in poly(APMP-co-MMA) for $f_{1,0} = 0.3$. For $f_{1,0} = 0.5$, the probability of unitary APMP or MMA was 73.0% and 82.8%, respectively. It was obtained that the alternating tendency prevailed. For $f_{1,0} = 0.7$, the probability of unitary MMA was 93.1%, which indicated that the APMP units were separated by the single MMA unit. While $f_{1,0}$ was further up to 0.9, the probability of unitary APMP was 12.3% and of APMP diads was 10.8%. The sequence of 10 units of APMP still had the probability of 3.8% existing in the backbone, where the sequential distribution was nearly opposite to the results from $f_{1,0} = 0.1$. It could be judged that the sequence distribution was affected by the feed ratios of APMP/MMA. When the APMP units dispersed in the copolymer chains equally, the copolymer could exhibit high ability to trap the radicals to protect the materials. The sequential distribution could be the guidance for the application of APMP derivatives as the light stabilizers.

4. Conclusion

The photoinduced copolymerization of APMP with MMA at ambient temperature was investigated. Both the rate of the photoinduced copolymerization and the average molecular weight increased with the increment of initial monomer feed ratio of APMP/MMA. The reaction kinetics of the copolymerization were linear. However, the WMD was irregular for nitroxide that was generated from APMP trapping

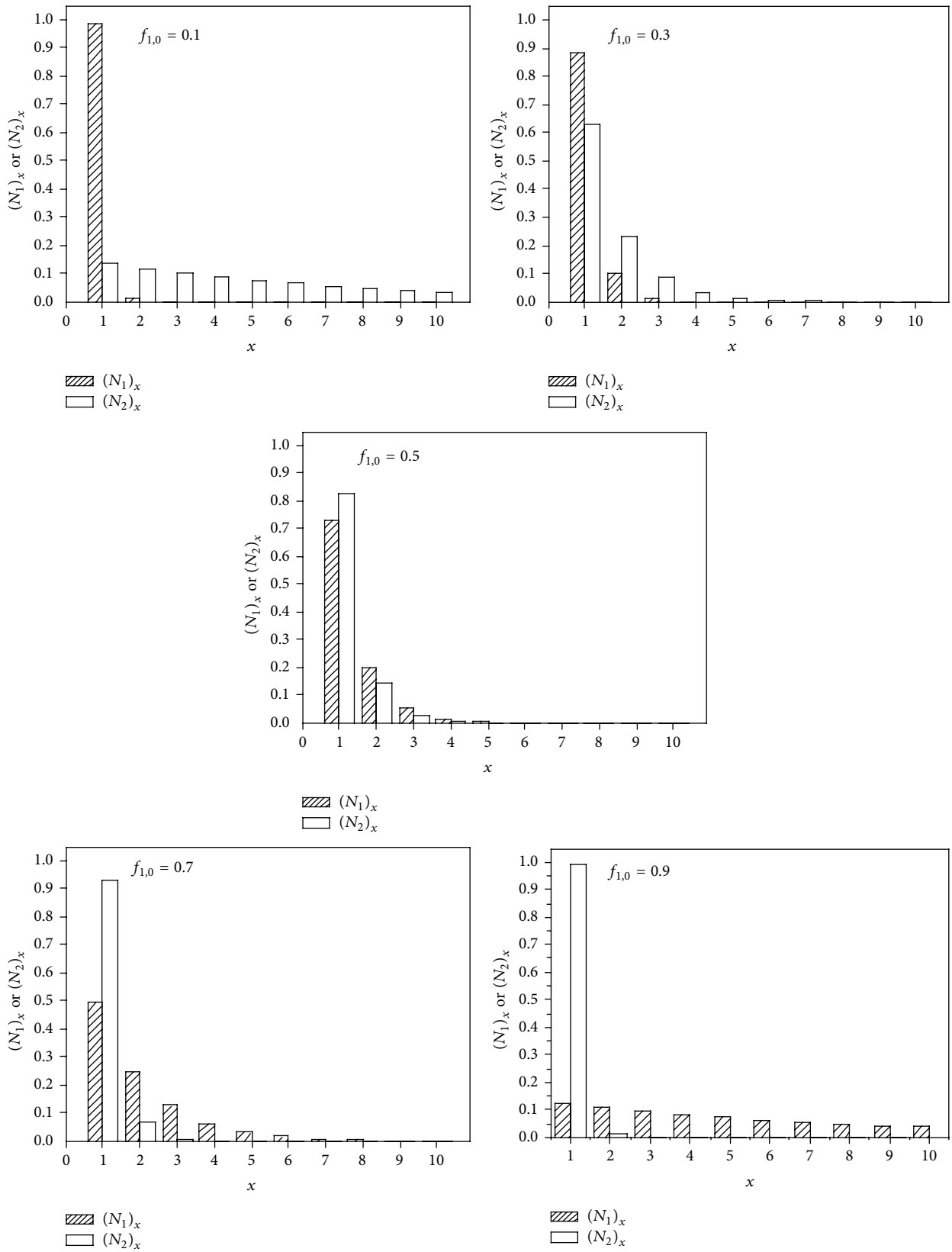

Figure 7: Sequence-length distributions of poly(APMP-co-MMA). $f_{1,0}$ = 0.1, 0.3, 0.5, 0.7, and 0.9. x was the number of sequence lengths of APMP/MMA unit. $(N_1)_x$ and $(N_2)_x$ were the probability APMP of and MMA unit in poly(APMP-*co*-MMA), respectively.

the propagating radicals to form branched dormant. The reactivity ratios of the copolymerization had been estimated by the data from ^{1}H NMR spectra, using the extended KT method at high conversions. The reactivity ratio for APMP and MMA was 0.353 and 0.168, respectively, which revealed that the resulting copolymer had a tendency toward alternation. Using the obtained reactivity ratios, a nonlinear model of the photoinduced copolymerization was established. The sequential distribution in poly(APMP-*co*-MMA) was also investigated, which was regulated by the feed ratios and reactivity ratios.

Competing Interests

The authors declare that they have no competing interests.

Acknowledgments

The project was financially supported by the National Natural Science Foundation of China (Grant no. 51403041).

References

[1] M. A. Tasdelen, M. Uygun, and Y. Yagci, "Photoinduced controlled radical polymerization," *Macromolecular Rapid Communications*, vol. 32, no. 1, pp. 58–62, 2011.

[2] E. Andrzejewska, "Photopolymerization kinetics of multifunctional monomers," *Progress in Polymer Science*, vol. 26, no. 4, pp. 605–665, 2001.

[3] X. Yang, L. Zhu, Y. Zhang et al., "Surface properties and self-cleaning ability of the fluorinated acrylate coatings modified with dodecafluoroheptyl methacrylate through two adding ways," *Applied Surface Science*, vol. 295, pp. 44–49, 2014.

[4] S. Atlas, M. Raihane, A. Hult, M. Malkoch, M. Lahcini, and B. Ameduri, "Radical copolymerization of acrylonitrile with 2,2,2-trifluoroethyl acrylate for dielectric materials: structure and characterization," *Journal of Polymer Science A: Polymer Chemistry*, vol. 51, no. 18, pp. 3856–3866, 2013.

[5] H. Yari, M. Mohseni, B. Ramezanzadeh, and A. M. Rabea, "Investigating the degradation resistance of silicone-acrylate containing automotive clearcoats exposed to bird droppings," *Progress in Organic Coatings*, vol. 75, no. 3, pp. 170–177, 2012.

[6] F. D. Jochum and P. Theato, "Temperature- and light-responsive smart polymer materials," *Chemical Society Reviews*, vol. 42, no. 17, pp. 7468–7483, 2013.

[7] J. Su, H. Huang, Y. Cui, Y. Chen, and X. Liu, "A photo-induced nitroxide trapping method to prepare α,ω-heterotelechelic polymers," *Polymer Chemistry*, vol. 7, no. 14, pp. 2511–2520, 2016.

[8] H. Yu, L. Cao, F. Li et al., "The antioxidant mechanism of nitroxide TEMPO: scavenging with glutathionyl radicals," *RSC Advances*, vol. 5, no. 78, pp. 63655–63661, 2015.

[9] K. Schwetlick and W. D. Habicher, "Antioxidant action mechanisms of hindered amine stabilisers," *Polymer Degradation and Stability*, vol. 78, no. 1, pp. 35–40, 2002.

[10] G. Gryn'ova, K. U. Ingold, and M. L. Coote, "New insights into the mechanism of amine/nitroxide cycling during the hindered amine light stabilizer inhibited oxidative degradation of polymers," *Journal of the American Chemical Society*, vol. 134, no. 31, pp. 12979–12988, 2012.

[11] G. I. Likhtenstein, K. Ishii, and S. I. Nakatsuji, "Dual chromophore-nitroxides: novel molecular probes, photochemical and photophysical models and magnetic materials," *Photochemistry and Photobiology*, vol. 83, no. 4, pp. 871–881, 2007.

[12] D. I. Pattison, M. Lam, S. S. Shinde, R. F. Anderson, and M. J. Davies, "The nitroxide TEMPO is an efficient scavenger of protein radicals: cellular and kinetic studies," *Free Radical Biology and Medicine*, vol. 53, no. 9, pp. 1664–1674, 2012.

[13] J. Nicolas, Y. Guillaneuf, C. Lefay, D. Bertin, D. Gigmes, and B. Charleux, "Nitroxide-mediated polymerization," *Progress in Polymer Science*, vol. 38, no. 1, pp. 63–235, 2013.

[14] F. Kato, A. Kikuchi, T. Okuyama, K. Oyaizu, and H. Nishide, "Nitroxide radicals as highly reactive redox mediators in dye-sensitized solar cells," *Angewandte Chemie—International Edition*, vol. 51, no. 40, pp. 10177–10180, 2012.

[15] M. Aydın, B. Esat, Ç. Kılıç, M. E. Köse, A. Ata, and F. Yilmaz, "A polythiophene derivative bearing TEMPO as a cathode material for rechargeable batteries," *European Polymer Journal*, vol. 47, no. 12, pp. 2283–2294, 2011.

[16] F. Gugumus, "Aspects of the impact of stabilizer mass on performance in polymers. 2. Effect of increasing molecular mass of polymeric HALS in PP," *Polymer Degradation and Stability*, vol. 67, no. 2, pp. 299–311, 2000.

[17] R. P. Singh, A. Vishwa Prasad, and J. K. Pandey, "Synthesis, characterization and performance evaluation of polymeric hindered amine light stabilizers in styrenic polymers," *Macromolecular Chemistry and Physics*, vol. 202, no. 5, pp. 672–680, 2001.

[18] G. J. Sun, H. J. Jang, S. Kaang, and K. H. Chae, "A new polymeric HALS: preparation of an addition polymer of DGEBA-HALS and its photostabilizing effect," *Polymer*, vol. 43, no. 22, pp. 5855–5863, 2002.

[19] L. Coulier, E. R. Kaal, M. Tienstra, and T. Hankemeier, "Identification and quantification of (polymeric) hindered-amine light stabilizers in polymers using pyrolysis-gas chromatography-mass spectrometry and liquid chromatography-ultraviolet absorbance detection-evaporative light scattering detection," *Journal of Chromatography A*, vol. 1062, no. 2, pp. 227–238, 2005.

[20] B. Xue and A. Toyota, "Synthesis of novel polymeric HALS stabilizers and chain transfer effect of hindered amine norbornene derivatives on ring-opening metathesis polymerization," *Polymer Bulletin*, vol. 62, no. 3, pp. 327–336, 2009.

[21] Y. Zhang, X. Liu, Z. Dong, and Y. Cui, "Study on photostabilization in situ of reactive hindered amine light stabilizers applied to UV-curable coatings," *Journal of Coatings Technology Research*, vol. 9, no. 4, pp. 459–466, 2012.

[22] A. R. Mahdavian, M. Abdollahi, L. Mokhtabad, H. R. Bijanzadeh, and F. Ziaee, "Kinetic study of radical polymerization. IV. Determination of reactivity ratio in copolymerization of styrene and itaconic acid by1H-NMR," *Journal of Applied Polymer Science*, vol. 101, no. 3, pp. 2062–2069, 2006.

[23] A. L. Holmberg, M. G. Karavolias, and T. H. Epps, "RAFT polymerization and associated reactivity ratios of methacrylate-functionalized mixed bio-oil constituents," *Polymer Chemistry*, vol. 6, no. 31, pp. 5728–5739, 2015.

[24] F. R. Mayo and F. M. Lewis, "Copolymerization. I. A basis for comparing the behavior of monomers in copolymerization; the copolymerization of styrene and methyl methacrylate," *Journal of the American Chemical Society*, vol. 66, no. 9, pp. 1594–1601, 1944.

[25] M. Fineman and S. D. Ross, "Linear method for determining monomer reactivity ratios in copolymerization," *Journal of Polymer Science*, vol. 5, no. 2, pp. 259–262, 1950.

[26] T. Kelen and F. Tüdős, "A new improved linear graphical method for determing copolymerization reactivity ratios," *Reaction Kinetics and Catalysis Letters*, vol. 1, no. 4, pp. 487–492, 1974.

[27] F. Tüdos, T. Kelen, T. Földes-Berezhnykh, and B. Turcsányi, "Evaluation of high conversion copolymerization data by a linear graphical method," *Reaction Kinetics and Catalysis Letters*, vol. 2, no. 4, pp. 439–447, 1975.

[28] T. Kelen, F. Tüdös, and B. Turcsányi, "Confidence intervals for copolymerization reactivity ratios determined by the Kelen-Tüdös method," *Polymer Bulletin*, vol. 2, no. 1, pp. 71–76, 1980.

[29] X. Liu, Y. Zhang, Y. Cui, and Z. Dong, "Reactivity ratios and sequence structures of the copolymers prepared using photoinduced copolymerization of MMA with MTMP," *Magnetic Resonance in Chemistry*, vol. 50, no. 5, pp. 372–378, 2012.

[30] Š. Chmela, P. Lajoie, P. Hrdlovič, and J. Lacoste, "Combined oligomeric light and heat stabilizers," *Polymer Degradation and Stability*, vol. 71, no. 1, pp. 171–177, 2000.

[31] X. Liu, J. Yang, and Y. Chen, "Reactive-HALS I: synthesis, characterization, copolymerization reactivity and photo-stabilizing performance applied in UV-curable coatings," *Polymers for Advanced Technologies*, vol. 13, no. 3-4, pp. 247–253, 2002.

[32] X. Liu, X. Zhang, X. Zhang et al., "Photoinduced controlled/living free-radical polymerization of 4-methacryloyl-1,2,2,6,6-pentamethyl-piperidenyl," *Journal of Polymer Science A: Polymer Chemistry*, vol. 42, no. 11, pp. 2659–2665, 2004.

[33] T. Okada and M. Otsuru, "A study of sequence distribution of chloroprene and methyl methacrylate copolymers by ^{1}H-NMR," *Journal of Applied Polymer Science*, vol. 23, no. 7, pp. 2215–2221, 1979.

[34] K. Hatada, T. Kitayama, Y. Terawaki et al., "NMR measurement of identical polymer samples by round robin method IV. Analysis of composition and monomer sequence distribution in poly(methyl methacrylate-co-acrylonitrile) leading to determinations of monomer reactivity ratios," *Polymer Journal*, vol. 27, no. 11, pp. 1104–1112, 1995.

[35] I. Skeist, "Copolymerization: the composition distribution curve," *Journal of the American Chemical Society*, vol. 68, no. 9, pp. 1781–1784, 1946.

[36] V. E. Meyer and G. G. Lowry, "Integral and differential binary copolymerization equations," *Journal of Polymer Science Part A: General Papers*, vol. 3, no. 8, pp. 2843–2851, 1965.

[37] M. T. Hunley and K. L. Beers, "Nonlinear method for determining reactivity ratios of ring-opening copolymerizations," *Macromolecules*, vol. 46, no. 4, pp. 1393–1399, 2013.